

Measurement of cross sections and oscillator strengths for Xe by electron impact

T. Y. Suzuki, Y. Sakai, B. S. Min, T. Takayanagi, K. Wakiya, and H. Suzuki
Department of Physics, Sophia University, Chiyoda-ku, Tokyo 102, Japan

T. Inaba and H. Takuma
Institute for Laser Science, University of Electro-Communications, Chofu-shi, Tokyo 182, Japan
 (Received 14 January 1991)

Differential cross sections and generalized oscillator strengths have been measured for two optically allowed transitions $5p^6(^1S_0) \rightarrow 5p^5(^2P_{1/2})6s$ and $5p^5(^2P_{3/2})6s$ in Xe by means of electron-energy-loss spectroscopy. These measurements are carried out for electron kinetic energies of 100, 400, and 500 eV at small scattering angles ($\theta = 1.4^\circ - 14.6^\circ$). The generalized oscillator strengths are extrapolated to zero momentum transfer to get the optical oscillator strengths and they are compared with those obtained by optical methods and theoretical calculations. The optical oscillator strengths obtained by this work for the $5p^5(^2P_{1/2})6s$ and $5p^5(^2P_{3/2})6s$ states are 0.158 ± 0.019 and 0.222 ± 0.027 , respectively. Integral cross sections have been also determined for each impact energy. The errors are estimated to be less than 12%.

I. INTRODUCTION

Reliable data of differential and integral cross sections for excitation of the resonance lines in rare-gas atoms by electron collisions are indispensable for the analyses of the energy convertibility in the rare-gas-hologen excimer lasers. We perform a series of measurements of the cross sections and oscillator strengths for the electron-impact excitation of the resonance lines in rare-gas atoms.

Measurements of differential cross sections (DCS's) and generalized oscillator strengths (GOS's) for resonance lines in argon and krypton have been previously published.^{1,2} In the present paper, the cross sections for Xe are reported from our laboratory.

There are a few theoretical calculations for the inelastic e -Xe scattering processes; Ganas and Green³ reported the calculation of the total excitation cross sections with an independent-particle model, including a distorted generalized oscillator strength method. As for experimental studies, the inelastic DCS's and the integral cross sections (ICS's) were given at 15-, 20-, 30-, and 80-eV impact energies by Filipovic *et al.*⁴ and at 20 eV by Williams, Trajmar, and Kuppermann.⁵ Nishimura, Danjo, and Matsuda⁶ reported some preliminary results. In the present work, the DCS's and the GOS's for the $5p^5(^2P_{1/2})6s$ and $5p^5(^2P_{3/2})6s$ states, which are designated as the $6s'[1/2]^\circ$ and $6s[3/2]^\circ$ according to the J - l coupling notation, respectively,⁷ are determined at 100-, 400-, and 500-eV impact energies by means of electron-energy-loss spectroscopy (EELS). The optical oscillator strengths (OOS's) and ICS's are also determined from the GOS's. The absolute DCS's and ICS's for 100-, 400-, and 500-eV impact energies are obtained in this paper.

II. EXPERIMENTAL PROCEDURES

The experimental apparatus has been described in the preceding papers on Ar and Kr.^{1,2} We use a simulated hemispherical-type electron-energy selector before the

scattering region to get a monoenergetic electron beam and we use the same type energy analyzer to analyze the scattered electrons.

The mean trajectory radius is 50 mm for the monochromator and 80 mm for the analyzer. The energy resolution of the apparatus is 50-meV full width at half maximum (FWHM) at 30-nA electron current, and 80 meV at 80 nA. All of these components are enclosed in a vacuum chamber (2×10^{-7} Torr).

The intensity of the scattered electrons decreases very rapidly with the scattering angle. So we use the entrance aperture at the analyzer of 0.5-mm diameter for small scattering angles ($\theta < 5^\circ$) and that of 1-mm diameter for large angles ($\theta > 5^\circ$) to save the signal accumulating time.

In the latter case, the angular resolution decreases, but it does not bring about large errors since the collision cross sections change more slowly in the large scattering region. The typical angular resolution was 0.4° (FWHM), at small scattering angles (40-nA electron current) and 0.8° at $\theta > 5^\circ$ (80 nA). They are determined by measuring the angular distribution of the direct electron beam from the energy selector.

The relative scattering intensities associated with elastic and inelastic scattering were determined from the corresponding peak areas of the energy-loss spectra in the scattering-angle region from 2° to 15° . Then the absolute DCS's are given from the relation

$$\left[\frac{d\sigma}{d\Omega} \right]_{\text{inel}} / \left[\frac{d\sigma}{d\Omega} \right]_{\text{el}} = \frac{I_{\text{inel}}}{I_{\text{el}}}, \quad (1)$$

where I is the intensity, and "inel" and "el" denote inelastic and elastic scattering, respectively. The actual zero-scattering angle has been calibrated using the symmetry nature of the intensity ratio $I_{\text{inel}}/I_{\text{el}}$ around 0° .

The $(d\sigma/d\Omega)_{\text{el}}$ were obtained by a calculation using a fitting function, which was based on the experimental data of the absolute elastic-scattering cross sections measured by Bromberg,⁸ Jansen and de Heer,⁹ and Wagenaar

*et al.*¹⁰ Using Eq. (1), the $(d\sigma/d\Omega)_{\text{inel}}$ can be determined by multiplying the ratio with the $(d\sigma/d\Omega)_{\text{el}}$. The generalized oscillator strength $F(K)$ is calculated from the formula¹

$$F(K) = \frac{Wk_i}{2k_f} K^2 \left[\frac{d\sigma}{d\Omega} \right], \quad (2)$$

where W is the excitation energy, k_i and k_f are the momenta of the colliding electrons before and after the collision, and K is the absolute value of the momentum-transfer vector. All quantities are in atomic units.

When the Born approximation holds, the GOS should be a function of K . The limit of the generalized oscillator strength at $K^2=0$ gives the OOS whether the Born approximation is valid or not. For the extrapolation of the experimental results to zero momentum transfer we have fitted the GOS values using the least-squares method with the polynomials of the form¹²

$$F(K) = \frac{1}{(1+x)^6} \left[f_0 + \sum_{n=1}^m f_n \left[\frac{1}{1+x} \right]^n \right], \quad (3)$$

where f_0 is the OOS, f_n are the coefficients, x is equal to $(K/Y)^2$, and Y is equal to $\sqrt{2I} + \sqrt{2(I-W)}$. Here I and W are the ionization energy and the excitation energy, respectively.

The ICS is obtained by integrating the measured DCS's over the whole angle using the following equation:

$$\sigma = 2\pi \int_0^\pi \left[\frac{d\sigma}{d\Omega} \right] \sin\theta d\theta. \quad (4)$$

At small angles, DCS's for the optically allowed transitions rise rapidly as the angle decreases; therefore the extrapolation to zero angle is difficult and unreliable. By transforming Eq. (2), the cross section is given by the equation

$$\frac{d\sigma}{d\Omega} = \frac{2}{WK^2} \left[\frac{k_f}{k_i} \right] F(K). \quad (5)$$

Changing the variable from 0 to K in Eq. (4) using Eq. (5) for the DCS, we get

$$\sigma = \frac{4\pi}{Wk_i^2} \int_{k_i-k_f}^{k_i+k_f} \frac{F(K)}{K} dK. \quad (6)$$

Because the K dependence of $F(K)$ is reasonably described by the formula of Eq. (3) in the present case, we make the numerical calculation according this formula.

III. RESULTS AND DISCUSSION

A typical energy-loss spectrum is shown in Fig. 1, which is taken at the impact energy of 400 eV and the scattering angle of 2.5°. The energy-loss peaks have been identified by a comparison with the spectroscopic values of the transition energies from a table compiled by Moore.⁷

An intense peak at 8.436 eV corresponds to the $5p^5(^2P_{3/2})6s$ excitation, while a peak at 9.570 eV corresponds to the $5p^5(^2P_{1/2})6s$ excitation. The latter peak in-

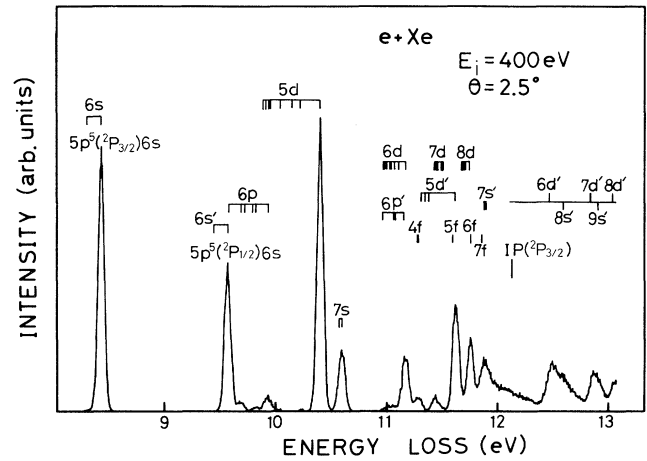


FIG. 1. A typical electron-energy-loss spectrum of Xe for the impact energy 400 eV at the scattering angle 2.5°.

cludes a contribution from the $5p^5(^2P_{3/2})6p$, $J=1$ forbidden transition. However, the $5p^5(^2P_{1/2})6s$ peak is large enough at small angles in comparison with these adjacent peaks of the forbidden transitions. The intensity ratios of the $5p^5(^2P_{1/2})6s$ and $5p^5(^2P_{3/2})6s$ peaks to the elastic scattering intensity are given in Table I.

The absolute elastic cross sections are obtained using a fitting function induced on the basis of the absolute elastic cross sections measured by Bromberg,⁸ by Jansen and de Heer,⁹ and by Wagenaar *et al.*¹⁰ In other words, we determine the $(d\sigma/d\Omega)_{\text{el}}$ by the interpolation and extrapolation of the experimental absolute elastic cross-section data. It is known that a curve of a semilogarithmic plot of $(d\sigma/d\Omega)_{\text{el}}$ against K shows a remarkable linear behavior in the region of small K .¹³ The elastic cross sections are fitted to a formula as follows:

$$\ln \left[\frac{d\sigma}{d\Omega} \right]_{\text{el}} = C_0 + C_1 K_0 + C_2 K_0^2 + C_3 K_0^3, \quad (7)$$

where K_0 is the momentum transfer and C_0 , C_1 , C_2 , and C_3 are the fitting parameters. Numerical results of $(d\sigma/d\Omega)_{\text{el}}$ are also listed in Table I.

The DCS's for the $5p^5(^2P_{3/2})6s$ and the $5p^5(^2P_{1/2})6s$ excitations are shown in Fig. 2 as functions of the scattering angle in the small-angle region. The DCS's for the $5p^5(^2P_{3/2})6s$ and the $5p^5(^2P_{1/2})6s$ transitions at 500 eV have a steeply forward-peaked angular dependence and possess a minimum at the scattering angle around 8.5°. The DCS's at 100 eV show a forward-peaked angular dependence, too, but they possess no minima in the scattering-angle region below 30°.

The GOS's for the two excitations processes are deduced using Eq. (2) and shown in Figs. 3 and 4. These GOS's fitted with the polynomials mentioned as the Eq. (3) are obtained as follows:

$$F_{3/2}(K) = \{ 0.222 - 1.374[x/(1+x)] + 1.484[x/(1+x)]^2 + 3.665[x/(1+x)]^3 + \dots \} / (1+x)^6, \quad (8)$$

TABLE I. The intensity ratios $(d\sigma/d\Omega)_{\text{inel}}/(d\sigma/d\Omega)_{\text{el}}$ for excitation of the $5p^5(^2P_{1/2})6s$ and the $5p^5(^2P_{3/2})6s$ states. The absolute elastic differential cross sections (in atomic units) at 100; 400-; and 500-eV impact energies are also listed. Square brackets denote powers of 10. The $(d\sigma/d\Omega)_{\text{el}}$ are given by the inter- and extrapolation of the results by Bromberg (Ref. 8), Jansen and de Heer (Ref. 9), and Wagenaar *et al.* (Ref. 10).

Angle (deg)	$\left(\frac{d\sigma}{d\Omega}\right)_{\text{el}}$ (a_0^2/sr)	Intensity ratio				$\left(\frac{d\sigma}{d\Omega}\right)_{\text{inel}}$ (units of a_0^2/sr)
		$^2P_{1/2}$	$^2P_{3/2}$	$^2P_{1/2}$	$^2P_{3/2}$	
$E_i = 100 \text{ eV}$						
2.45	1.53[2]	1.58[-1]	2.91[-1]	2.41[1]	4.44[1]	
2.95	1.40[2]	1.46[-1]	2.60[-1]	2.04[1]	3.63[1]	
3.05	1.38[2]	1.40[-1]	2.46[-1]	1.93[1]	3.38[1]	
3.45	1.29[2]	1.28[-1]	2.19[-1]	1.64[1]	2.81[1]	
3.55	1.26[2]	1.20[-1]	2.15[-1]	1.51[1]	2.72[1]	
3.95	1.18[2]	1.13[-1]	1.96[-1]	1.34[1]	2.32[1]	
4.05	1.16[2]	1.06[-1]	1.78[-1]	1.23[1]	2.07[1]	
4.45	1.08[2]	9.92[-2]	1.65[-1]	1.08[1]	1.79[1]	
4.55	1.07[2]	8.84[-2]	1.54[-1]	9.42[0]	1.64[1]	
4.95	9.97[1]	8.91[-2]	1.43[-1]	8.87[0]	1.45[1]	
5.45	9.16[1]	7.90[-2]	1.25[-1]	7.24[0]	1.14[1]	
5.55	9.00[1]	7.14[-2]	1.18[-1]	6.43[0]	1.06[1]	
6.55	7.60[1]	6.16[-2]	9.40[-2]	4.68[0]	7.14[0]	
8.55	5.33[1]	3.39[-2]	5.23[-2]	1.81[0]	2.79[0]	
12.55	2.58[1]	1.05[-2]	1.54[-2]	2.70[-1]	3.69[-1]	
16.55	1.07[1]	6.85[-3]	8.62[-3]	7.33[-2]	9.22[-2]	
20.55	3.50[0]	1.06[-2]	1.95[-2]	3.72[-2]	6.82[-2]	
24.55	9.79[-1]	3.38[-2]	5.03[-2]	3.30[-2]	4.93[-2]	
28.55	3.36[-1]	6.05[-2]	8.98[-2]	2.03[-2]	3.02[-2]	
32.55	2.95[-1]	1.30[-2]	1.79[-2]	3.84[-3]	5.30[-3]	
$E_i = 400 \text{ eV}$						
1.4	1.69[2]	2.06[-1]	3.39[-1]	3.47[1]	5.72[1]	
1.6	1.61[2]	1.72[-1]	2.78[-1]	2.77[1]	4.48[1]	
1.9	1.51[2]	1.35[-1]	2.14[-1]	2.04[1]	3.24[1]	
2.1	1.45[2]	1.13[-1]	1.81[-1]	1.63[1]	2.62[1]	
2.4	1.35[2]	9.08[-2]	1.45[-1]	1.23[1]	1.96[1]	
2.6	1.30[2]	7.68[-2]	1.21[-1]	9.96[0]	1.57[1]	
2.9	1.22[2]	6.35[-2]	1.02[-1]	7.72[0]	1.24[1]	
3.1	1.17[2]	5.37[-2]	8.45[-2]	6.26[0]	9.85[0]	
3.4	1.09[2]	4.53[-2]	7.21[-2]	4.96[0]	7.89[0]	
3.6	1.05[2]	3.72[-2]	5.81[-2]	3.90[0]	6.09[0]	
3.9	9.86[1]	3.09[-2]	4.74[-2]	3.04[0]	4.68[0]	
4.4	8.90[1]	2.22[-2]	3.46[-2]	1.97[0]	3.08[0]	
4.6	8.54[1]	1.92[-2]	2.87[-2]	1.64[0]	2.45[0]	
5.4	7.26[1]	1.13[-2]	1.68[-2]	8.23[-1]	1.22[0]	
5.6	6.97[1]	1.06[-2]	1.46[-2]	7.41[-1]	1.02[0]	
6.6	5.70[1]	5.34[-3]	6.62[-3]	3.04[-1]	3.77[-1]	
7.6	4.65[1]	2.42[-3]	2.99[-3]	1.12[-1]	1.39[-1]	
$E_i = 500 \text{ eV}$						
1.5	1.63[2]	1.56[-1]	2.50[-1]	2.54[1]	4.06[1]	
2.0	1.45[2]	1.05[-1]	1.70[-1]	1.52[1]	2.46[1]	
2.5	1.29[2]	6.59[-2]	1.01[-1]	8.52[0]	1.31[1]	
3.0	1.16[2]	4.51[-2]	6.79[-2]	5.22[0]	7.85[0]	
3.5	1.04[2]	2.91[-2]	4.46[-2]	3.02[0]	4.63[0]	
4.0	9.34[1]	1.89[-2]	2.88[-2]	1.76[0]	2.69[0]	
4.5	8.41[1]	1.32[-2]	1.86[-2]	1.11[0]	1.56[0]	
5.2	7.27[1]	7.46[-3]	1.09[-2]	5.42[-1]	7.91[-1]	
5.5	6.84[1]	5.71[-3]	8.85[-3]	3.90[-1]	6.05[-1]	
6.2	5.93[1]	2.87[-3]	3.80[-3]	1.70[-1]	2.25[-1]	
7.2	4.83[1]	1.25[-3]	1.50[-3]	6.04[-2]	7.25[-2]	
8.2	3.92[1]	5.04[-4]	6.29[-4]	1.98[-2]	2.47[-2]	
8.6	3.60[1]	4.71[-4]	6.95[-4]	1.70[-2]	2.50[-2]	

TABLE I. (Continued).

Angle (deg)	$\left(\frac{d\sigma}{d\Omega}\right)_{el}$ (a_0^2/sr)	Intensity ratio		$\left(\frac{d\sigma}{d\Omega}\right)_{inel}$ (units of a_0^2/sr)	
		${}^2P_{1/2}$	${}^2P_{3/2}$	${}^2P_{1/2}$	${}^2P_{3/2}$
$E_i = 500$ eV					
9.6	2.90[1]	7.70[-4]	1.14[-3]	2.23[-2]	3.30[-2]
10.6	2.31[1]	9.12[-4]	1.41[-3]	2.11[-2]	3.26[-2]
11.6	1.81[1]	1.22[-3]	1.81[-3]	2.22[-2]	3.29[-2]
12.6	1.40[1]	1.26[-3]	1.80[-3]	1.76[-2]	2.52[-2]
13.6	1.06[1]	1.17[-3]	1.71[-3]	1.24[-2]	1.82[-2]
14.6	7.90	1.08[-3]	1.73[-3]	8.54[-3]	1.37[-2]

$$F_{1/2}(K) = \{0.158 - 0.575[x/(1+x)] - 1.227[x/(1+x)]^2 + 5.935[x/(1+x)]^3 + \dots\} / (1+x)^6$$

(determined at 400 and 500 eV), (9)

$$F_{3/2}(K) = \{0.222 - 1.204[x/(1+x)] - 3.980[x/(1+x)]^2 + 30.49[x/(1+x)]^3 + \dots\} / (1+x)^6, \quad (10)$$

$$F_{1/2}(K) = \{0.158 - 0.404[x/(1+x)] - 4.429[x/(1+x)]^2 + 11.84[x/(1+x)]^3 + \dots\} / (1+x)^6$$

(determined at 100 eV). (11)

In the graph of GOS versus K^2 , the data points taken at 400 and 500 eV lie on the same curves. In the region of small K^2 ($K^2 < 0.1$), data points taken at 100 eV also lie on the same curves. But at $K^2 > 0.15$ they begin to be smaller than those of 400 and 500 eV. And the larger K^2

is, the larger these discrepancies become. This shows that, at 100-eV impact energy, the Born approximation holds only in the region of small K^2 .

The presence of a minimum in the GOS versus K^2 curve for the $5p^5({}^2P_{3/2})6s$ transition in Xe was observed experimentally and calculated theoretically by Kim *et al.*¹⁴ In the present experiment, the existence of the minimum for both the $5p^5({}^2P_{3/2})6s$ and the $5p^5({}^2P_{1/2})6s$ transitions is observed. A comparison of the present GOS for the $5p^5({}^2P_{3/2})6s$ transition with those by Kim *et al.* is shown in Fig. 5. It is obviously found that our GOS's are slightly larger than those calculated by Kim *et al.* over the whole range of K^2 , but there exists a satisfactory agreement between the two in a shape of the curve. Moreover, our results reproduce very well the experimental ones for the impact energy 400 eV at large K^2

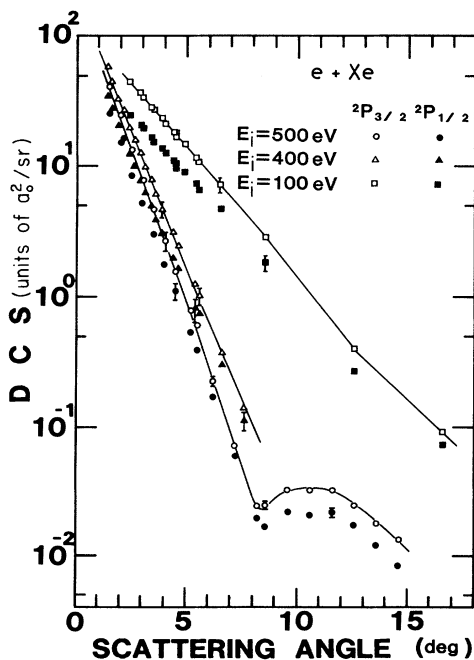


FIG. 2. Absolute differential cross sections for the excitation of the $5p^5({}^2P_{1/2})6s$ and the $5p^5({}^2P_{3/2})6s$ states in Xe as a function of the scattering angle.

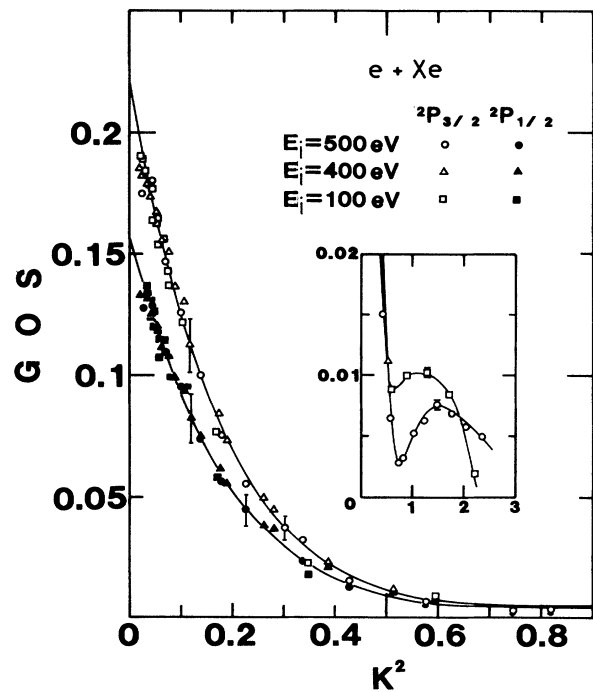


FIG. 3. The generalized oscillator strengths for the $5p^5({}^2P_{1/2})6s$ and the $5p^5({}^2P_{3/2})6s$ states in Xe as a function of the squared momentum transfer K^2 . Solid lines are calculated by Eqs. (8) and (9). Inset shows an enlarged plot in the vicinity of the minimum.

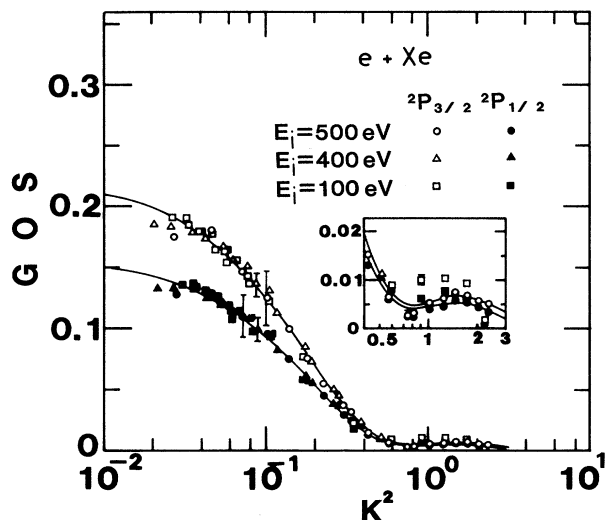


FIG. 4. The generalized oscillator strengths for the $5p^5(^2P_{1/2})6s$ and the $5p^5(^2P_{3/2})6s$ states in Xe as a function of the logarithm of the K^2 . The same symbols and notations are used as Fig. 3.

($K^2 > 0.1$) reported by Kim *et al.*, especially in the region of the minimum and the maximum of the GOS. It is known that the GOS must have a zero value at the minimum if the Born approximation is to strictly hold.¹⁴ However, the present GOS has finite values at the minimum; we suggest that there occurs a substantial deviation from the Born approximation in the vicinity of K^2 , for which the GOS has the minimum value. This deviation becomes larger as the impact energy decreases. A similar feature has been already reported for the $6^1S_0 \rightarrow 6^1P_1$ transition in mercury by Skerbele and

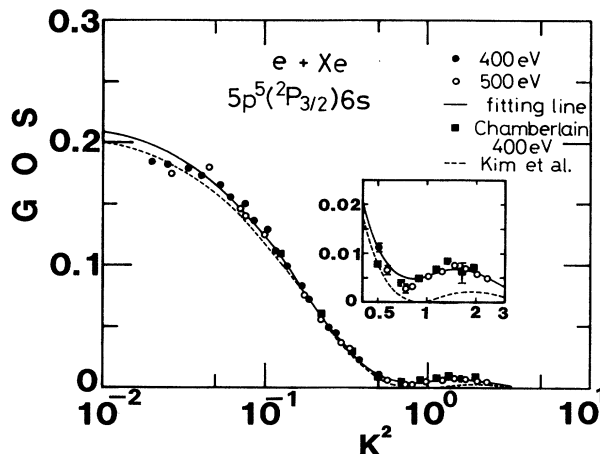


FIG. 5. A comparison of the present generalized oscillator strengths for the $5p^5(^2P_{3/2})6s$ with the results of Kim *et al.* (Ref. 14). The solid line is calculated by Eq. (8). Solid squares are experimental data by Kim *et al.* for the impact energy 400 eV. The dashed line is a calculated curve of Kim *et al.*

Lassette,¹⁵ and calculated using the distorted-wave approximation by Sawada, Purcell, and Green.¹⁶

The present results of the OOS are compared with the published data in Table II. Moreover, the ratios of the OOS for the $5p^5(^2P_{3/2})6s$ state to the $5p^5(^2P_{1/2})6s$ state determined from the present work are compared with other available data. The experimental absolute OOS were reported by Anderson¹⁷ using the zero-field level-crossing method, by Wilkinson¹⁸ using the optical-absorption technique, by Lu¹⁹ and Delage and Carette²⁰ using the low-energy electron impact, and by Geiger²¹ and Brion²² using the high-energy electron impact. The

TABLE II. Comparison of the present optical oscillator strengths for the $5p^5(^2P_{1/2})6s$ and the $5p^5(^2P_{3/2})6s$ states in Xe with those of previous authors.

Author	$^2P_{1/2}$	OOS	$^2P_{3/2}$	Ratio in the OOS $^2P_{3/2}/^2P_{1/2}$
EELS				
This work	0.158 ± 0.019		0.222 ± 0.027	1.41
K.T. Lu ^a	0.189		0.272	1.44
J. Geiger ^b	0.19		0.260	1.37
A. Delage ^c	0.169		0.183	1.08
C. E. Brion ^d	0.173		0.252	1.46
Optical measurements				
Anderson ^e	0.238		0.256	1.08
Wilkinson ^f	0.260		0.270	1.04
Calculations				
Dow and Knox ^g	(A) 0.147		0.194	1.32
	(B) 0.170		0.190	1.12
Kim <i>et al.</i> ^h	0.189		0.212	1.12

^aReference 19.

^bReference 21.

^cReference 20.

^dReference 22.

^eReference 17.

^fReference 18.

^gReference 23.

^hReference 14.

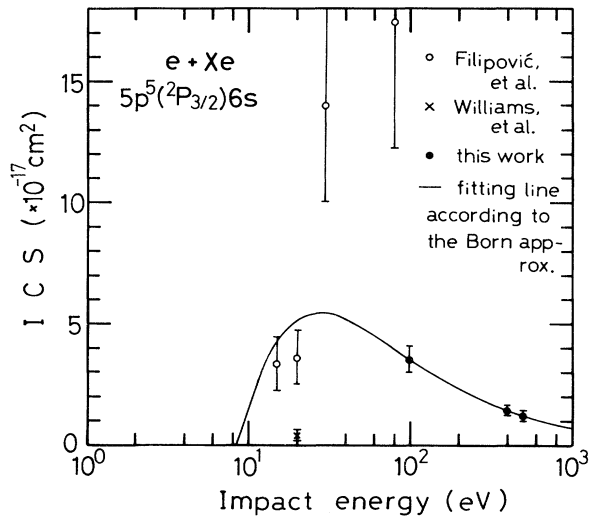


FIG. 6. Integral cross section for the $5p^5(^2P_{3/2})6s$ state as a function of the impact energy. The solid circles are the present results and the solid curve is derived from Eqs. (6) and (8), i.e., the integral cross section is deduced in terms of the Born approximation. The open circles are experimental results of Filipović *et al.* (Ref. 4) and the cross is by Williams, Trajmar, and Kuppermann (Ref. 5).

OOS's were also determined by Dow and Knox²³ using a theoretical calculation based on a wave function (A) and experimental energies, and the dipole matrix computed from the wave function (B), and by Kim *et al.* from the Hartree-Fock wave functions.

Our absolute values of the OOS are slightly smaller than other experimental values. The same situation occurs for the Kr $4p^5(^2P_{1/2,3/2})5s$ excitations but recent results of Tsurubuchi, Watanabe, and Arikawa²⁴ agree with ours to within the experimental errors. The ratios of the OOS for the $5p^5(^2P_{3/2})6s$ to the $5p^5(^2P_{1/2})6s$ agree well with the values of Lu and Brion.

The ICS's at 100-, 400-, and 500-eV impact energies are determined using Eq. (6) and tabulated in Table III. From the GOS's at 400- and 500-eV impact energies, ICS's at lower impact energies can be calculated within the framework of the Born approximation. These results are shown in Figs. 6 and 7, where experimental values determined by Williams, Trajmar, and Kupperman⁵ and Filipović *et al.*⁴ are also presented for comparison. It is well known that the Born approximation gives cross sections close to the experiments at higher impact energies,

TABLE III. Integrated cross sections for the excitation of the $5p^5(^2P_{1/2})6s$ and the $5p^5(^2P_{3/2})6s$ states in Xe.

Impact energy (eV)	Cross section (10^{-17} cm ²)	
	$^2P_{1/2}$	$^2P_{3/2}$
100	2.04 ± 0.25	3.52 ± 0.42
400	0.879 ± 0.11	1.48 ± 0.18
500	0.751 ± 0.09	1.26 ± 0.15

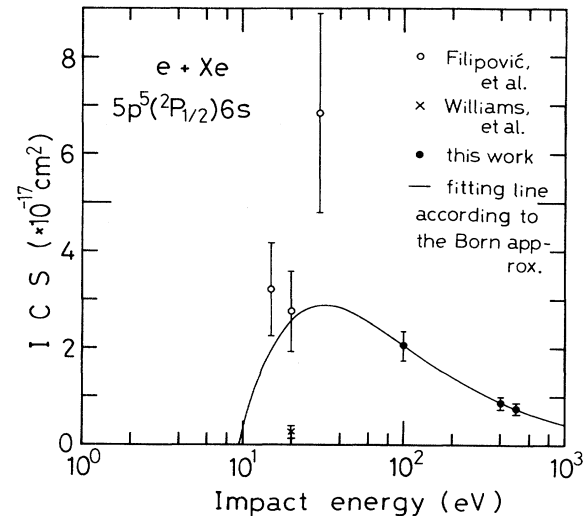


FIG. 7. Integral cross sections for the $5p^5(^2P_{1/2})6s$ state as a function of the impact energy. The same symbols and notations are used in Fig. 6.

while it gives cross sections too large compared with experiments at lower energies. For the $5p^5(^2P_{3/2})6s$ excitation, the results of Filipović *et al.*⁴ at 15- and 20-eV impact energies seem to be reasonable ones for the reason mentioned above. But the results at 30 and 80 eV are too large in view of the present discussion. For the

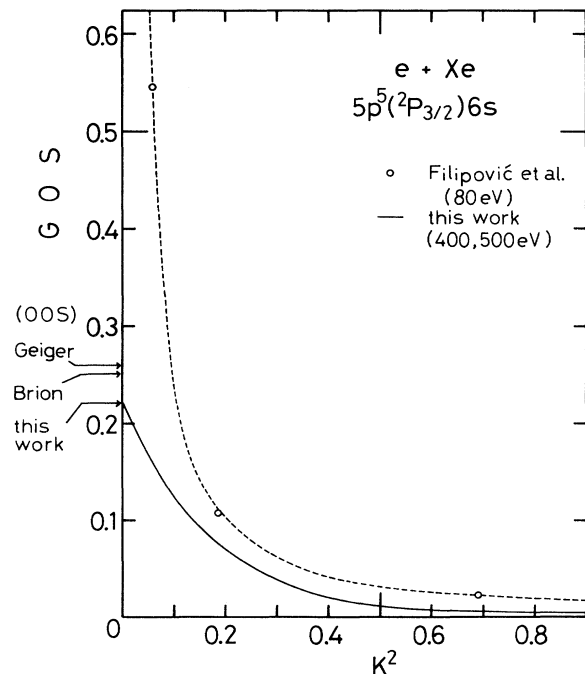


FIG. 8. Effective generalized oscillator strengths for the $5p^5(^2P_{3/2})6s$ state. The solid line is the present results deduced using Eq. (8). Open circles and a dashed line are transformed from the DCS's for 80-eV impact energy measured by Filipović *et al.* (Ref. 4).

$5p^5(^2P_{1/2})6s$ transition, all results (at 15, 20, and 30 eV) are larger than ours. In order to investigate the cause of these discrepancies, the DCS's for the $5p^5(^2P_{3/2})6s$ transition at 80 eV, where the Born approximation is expected to be not so bad in analogy with our results at 100 eV, were transformed to the GOS and compared with the present GOS. This is shown in Fig. 8.

The GOS's of Filipovic *et al.* at small K^2 are unduly larger than our OOS and all data reported. When we consider that the GOS approaches the OOS in the limit of $K \rightarrow 0$, it seems that their GOS's at small K^2 are quite unreasonable. We cannot help but conclude that their DCS's at small angles are too large and that they mainly contribute to the erroneous results.

The ICS's for both the $5p^5(^2P_{3/2})6s$ and the $5p^5(^2P_{1/2})6s$ transitions obtained by Williams, Trajmar, and Kuppermann⁵ are much smaller than those of ours. This discrepancy is considered to be due to the normalization procedure that is based on the systematically small total cross-section values measured by the Ramsauer technique, as pointed out by Filipovic *et al.*⁴

The systematic errors in the measured DCS's due to the effect of the limited angular resolution are negligibly small in the present experiment. In the preceding work for Ar and Kr,^{1,2} there existed systematic errors of about +5% due to the insufficient angular resolution (0.8° FWHM). In the present experiment, the angular resolution is improved to 0.4° (FWHM) at the angular region below 5°, which suppresses the undesirable effect of the limited angular resolution. The errors in the results of the DCS's and GOS's are estimated to be 7%. The uncertainties in the OOS are estimated to be 12% as the quadratic sum of the errors of the GOS's (7%) and the errors induced in the extrapolation procedure of the GOS (10%). The errors in the ICS's are also of a similar extent.

ACKNOWLEDGMENT

The present work is partly supported by a grant-to-aid from the Ministry of Education, Science and Culture of Japan.

¹G. P. Li, T. Takayanagi, K. Wakiya, H. Suzuki, T. Ajiro, S. Yagi, S. S. Kano, and H. Takuma, *Phys. Rev. A* **38**, 1240 (1988).

²T. Takayanagi, G. P. Li, K. Wakiya, H. Suzuki, T. Ajiro, T. Inaba, S. S. Kano, and H. Takuma, *Phys. Rev. A* **41**, 5948 (1990).

³P. S. Ganas and A. E. S. Green, *Phys. Rev. A* **4**, 182 (1971).

⁴D. Filipovic, B. Marinkovic, V. Pejcev, and L. Vuskovic, *Phys. Rev. A* **37**, 356 (1988).

⁵W. Williams, S. Trajmar, and A. Kuppermann, *J. Chem. Phys.* **62**, 3031 (1975).

⁶H. Nishimura, A. Danjo, and T. Matsuda, in *Abstracts of Contributed Papers of the Fourteenth International Conference on the Physics of Electronic and Atomic Collision, Palo Alto, 1985*, edited by M. J. Coggiola, D. L. Huestis, and R. P. Saxton (ICPEAC, Palo Alto, 1985), p. 108.

⁷C. E. Moore, *Atomic Energy Levels*, Natl. Bur. Stand. (U.S.) Circ. No. 467 (U.S. GPO, Washington, D.C., 1958), Vol. III.

⁸J. P. Bromberg, *J. Chem. Phys.* **61**, 963 (1974).

⁹R. H. J. Jansen and F. J. de Heer, *J. Phys. B* **9**, 213 (1976).

¹⁰R. W. Wagenaar, A. de Boer, T. van Tubergen, J. Los, and F. J. de Heer, *J. Phys. B* **19**, 3121 (1986).

¹¹H. Bethe, *Ann. Phys. (Leipzig)* **5**, 325 (1930).

¹²K. N. Klump and E. N. Lassette, *J. Chem. Phys.* **68**, 886 (1978).

¹³R. H. Jansen, F. J. de Heer, H. J. Luyken, B. van Wingerden, and H. J. Blaauw, *J. Phys. B* **9**, 185 (1976).

¹⁴Y. K. Kim, M. Inokuti, G. E. Chamberlain, and S. R. Mielczarek, *Phys. Rev. Lett.* **21**, 1146 (1968).

¹⁵A. Skerbele and E. N. Lassette, *J. Chem. Phys.* **58**, 2887 (1973).

¹⁶T. Sawada, J. E. Purcell, and A. E. S. Green, *Phys. Rev. A* **4**, 193 (1971).

¹⁷D. K. Anderson, *Phys. Rev.* **137**, A21 (1965).

¹⁸P. G. Wilkinson, *J. Quant. Spectrosc. Radiat. Transfer* **6**, 823 (1966).

¹⁹K. T. Lu, *Phys. Rev. A* **4**, 579 (1971).

²⁰A. Delage and J. D. Carette, *Phys. Rev. A* **14**, 1345 (1976).

²¹J. Geiger, in *Proceedings of the Fourth International Conference on Vacuum Ultraviolet Radiation Physics, Hamburg, 1974*, edited by E. E. Koch, R. Haensel, and R. Kunz (Pergamon, New York, 1974), p. 28.

²²C. E. Brion (private communication).

²³J. D. Dow and R. S. Knox, *Phys. Rev.* **152**, 50 (1966).

²⁴S. Tsurubuchi, K. Watanabe, and T. Arikawa, *J. Phys. B* **22**, 2969 (1989).